PHYSICSAccess Research Paper
ISSN Online: 2756-3898, ISSN Print: 2714-500X https://doi.org/10.47514/phyaccess.sp.iss.2022.1.003

First Principle Investigation on Electronic Properties of Cationic and Anionic CO-Alloyed Cu_2ZnSnS_4 Kesterite Material

Aliyu A Masanawa[1], Alhassan Shuaibu[2], Muhammed M Aliyu[2] and Ismail Magaji[2]

[1] Department of Science Laboratory, Kaduna Polytechnic, Kaduna, Kaduna State, Nigeria
[2] Department of Physics, Kaduna State University, Kaduna, Kaduna State, Nigeria

Corresponding E-mail: alhazikara@gmail.com

Received 07-10-2022
Accepted for publication 03-11-2022
Published 08-11-2022

Abstract

The primary goal of kesterite alloying is to allow for fine tweaking of the material's characteristics for advanced device engineering. Additionally, it is seen as a viable solution to inherent kesterite absorber difficulties such as the Cu/Zn disorder or Sn multivalency. The most interesting alloying elements for kesterite are Ag replacing Cu, Cd replacing Zn, and Ge replacing Sn for cationic substitution, as well as Se replacing S for anionic substitution. This research work investigates the effect of alloying CZTS with Silver (Ag) (Cation) and Selenium (Se) (Anion) theoretically using Density Functional Theory (DFT). The compounds were found to exhibit indirect bandgap characteristics, with conduction band minima (CBM) and valence band maxima (VBM) located between the N and gamma points of the Brillouin zone for pure kesterite Cu_2ZnSnS_4 and between the N and A points for alloyed $Ag_2ZnSnSe_4$ respectively. The bandgap of around 1.22 eV and 0.78 eV were recorded for the pure and alloyed kesterite materials. From the obtained results, a shrink in bandgap was observed due to the presence of heavy anion (Se) and cation (Ag) alloying at the same time. It was also found that the contribution of different atomic orbitals to the formation of the valence and conduction bands is approximately identical for pure and alloyed materials.

Keywords: Kesterite material; Density Functional Theory; Bandgap; Photovoltaic; Alloying

I. INTRODUCTION

Globally, research into renewable energy sources, including photovoltaic (PV) solar cells, is ongoing to fulfill growing energy demand and combat climate change. The use of chalcogenide materials such as $Cu(In,Ga)(S,Se)_2$ as the absorber layer in solar cells has garnered significant interest from the scientific community over the last 40 years, culminating in a world record efficiency of 23.35% in January, 2019 [1]. Recently, a family of similar compounds known as kesterite materials enabled the accomplishment of efficiencies ranging from 10% to 12.6% [2]. This material family is demonstrated to be a good contender for low-cost, abundant-on-earth, high-efficiency solar cells. In 2011, the European Commission (EC) announced interest in technologies that do not require 'Critical Raw Materials' (CRM). The EC produced a peer-reviewed list of CRMs in 2017 that included Ga and In [3].

Historically, due to the structural similarities between kesterite and chalcopyrite compounds, the typical device construction for $Cu(In,Ga)(S,Se)_2$ (CIGSSe) was immediately extended to CZTSSe by simply substituting a p-type CZTSSe thin film for the CIGSSe absorber layer. Typically, CZTSSe solar cells are manufactured on soda-lime glass (SLG)

substrate covered with a sputtered Mo layer to serve as the rear metallic contact. Typical sputter-deposited Mo layer thickness is around 500 nm up to 1 μm [4]. After that, the kesterite absorber is placed on top of the Mo layer. The quaternary systems, Cu-Zn-Sn-S and Cu-Zn-Sn-Se, are derived from CIS by substitution of two In atoms for one Zn and one Sn atom. This is called isoelectronic substitution and it produces a material with many of the same properties as the parent compound except that it no longer includes the expensive element. This new material still maintains a p-type conductivity and a high absorption coefficient (Absorption coefficient = $\alpha > 10^4$ cm^{-1}, equivalent to 90% of the incident light being absorbed to the surface within 100 nm) [5]. The sulfide compound has a bandgap of 1.5 eV, and the selenide compound has a bandgap of 0.96 eV [6]. The alloying of CZTS and CZTSe to form a pentenary system allows for tuning of the material's bandgap based on the sulfur to selenium ratio. Another advantage of the similarity between this material and CIS is that CZTSSe can be directly substituted into the standard thin film device structure.

Quaternary CZTS with I2-II-IV-VI4 structure can be derived from CIS by replacing In^{3+} with Zn^{2+} and Sn^{4+}. As long as the octet rule is satisfied, it is possible to derive several ternary/quaternary semiconductor materials, including $CuInS_2$, $CuGaS_2$, $CuFeS_2$, Cu_2ZnSnS_4, Cu_2FeSnS_4, Cu_2CdSnS_4, Cu_2ZnGeS_4 and their selenide counterparts [5].

It has been shown theoretically and experimentally that tetragonal kesterite is the most stable crystal structure for $Cu_2ZnSn(S,Se)_4$ although several metastable structures including stannite, Zinc blende, wurtzite, wurtzite-kesterite and wurtzite-stannite have also been observed. Kesterite CZTS has a direct bandgap of 1.5 eV and a high absorption coefficient (>10^4) which is close to the ideal for a single-junction solar cell. The bandgap can also be tuned by altering the S/Se ratio between 1.0 eV for pure selenide and 1.5 eV for pure sulfide compounds [7].

The scope of this research is to theoretically investigate the model of CTZS by replacing the copper (Cu) with Silver (Ag) for cation alloying, as well as Selenium (Se) replacing Sulphur (S) for anionic alloying. It will be limited to calculating the electronic property of both the pure Cu_2ZnSnS_4 and Co-Alloyed $Ag_2ZnSnSe_4$ Kesterite within the Density functional theory (DFT).

II. METHODS

The calculations were performed on a super-cell structure relative to the standard conventional unit cell compounds, using first principle calculation by Quantum ESPRESSO simulation package code within DFT. Within the Perdew-Burke-Ernzerhof generalized gradient approximation (PBE-GGA) [8], a pseudo potential was utilized to approximate the exchange-correlation potential for both pure Cu_2ZnSnS_4 and alloyed $Ag_2ZnSnSe_4$ Kesterite. The Maxfessel-Paxton smearing method, was used for integrals, while the Monkhorst-Pack technique was used to integrate the Brillouin zone [9], with 10×10×1 and 12×12×1 k-points grids for the pure and alloyed compound respectively.

For alloying in the Copper atomic site, all the copper atoms in the cells were replaced with Ag as cation alloyed and all the sulphur atoms were replaced with Selenium as anion alloyed. The cell dimensions are constant throughout the calculations; however, the atomic locations are completely loosened for all calculations using Broyden-Fletcher-Golfarb-Shanno (B.F.G.S.) algorithms, until the forces acting on the atoms were less than 0.001 eV [10].

III. RESULTS AND DISCUSSION

A. Electronic Band Structure

Electronic band structure calculated along the high symmetric point's Γ→H→N→Γ→A in irreducible Brillouin for the pure kesterite Cu_2ZnSnS_4 and alloyed $Ag_2ZnSnSe_4$ are shown in Fig. 1, with Fermi level at 0 eV.

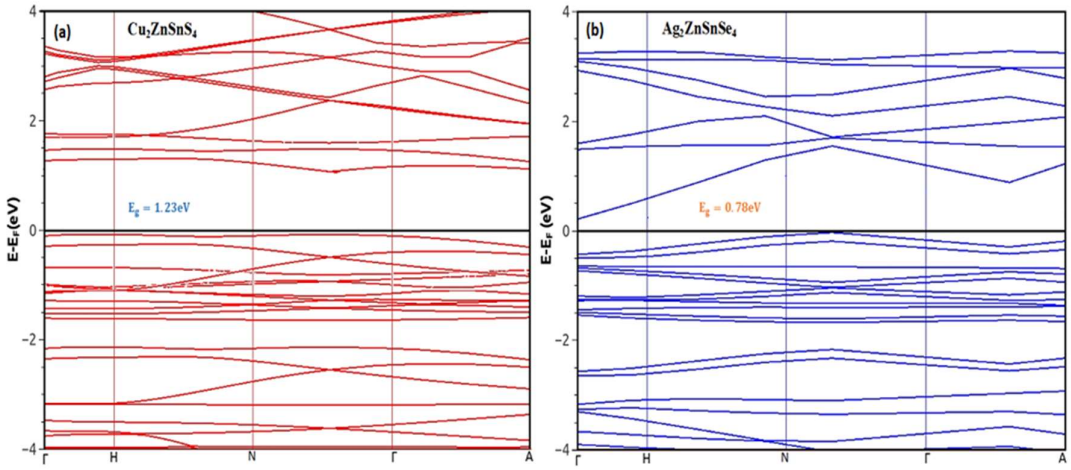

Fig. 1 (a) Calculated Band structure of pure kesterite Cu_2ZnSnS_4 (b) of Alloyed $Ag_2ZnSnSe_4$

The values of the respective band gaps are clearly indicated in Fig. 1 for each of the related band configurations. The graph's entire negative energy region corresponds to the valance band, whereas the positive energy portion corresponds to the conduction band. Both systems exhibited indirect bandgap characteristics, with conduction band minima (CBM) and valence band maxima (VBM) located between the N and gamma points of the Brillouin zone for pure kesterite Cu_2ZnSnS_4 and between the N and A points for alloyed $Ag_2ZnSnSe_4$ respectively. In pure kesterite Cu_2ZnSnS_4, a larger bandgap of around 1.22 eV was discovered; this value is consistent with [6] and is similar to some other pure kesterite systems as reported by [11], while the alloyed system exhibits a relatively smaller bandgap of about 0.78 eV as compared to pure kesterite. The observed shrink in bandgap due to the presence of heavy anion (Se) and cation (Ag) alloying at the same time is because VBM of the pure Cu_2ZnSnS_4 is formed of hybridized Cu 3d states and S p states, the presence of Ag-3d and Se p states would undoubtedly affect the shrinkage. This demonstrates unequivocally that the lighter atomic levels in heavier anions and cations contribute to VBM at higher states, hence lowering the bandgap [12, 13]. This estimated band gap value for the alloyed is found to be smaller than the bandgap values empirically observed for certain similar alloyed kesterite. However, this is consistent with previously published band gap estimates derived from density functional theory.

To gain a better understanding of the electronic properties, the total and partial density of states (DOS) for pure kesterite Cu_2ZnSnS_4 and alloyed $Ag_2ZnSnSe_4$ were calculated and displayed in Fig. 2 within the energy range of -6 eV to 6 eV, thereby validating the calculated electronic band structure. As observed in the graph, the contribution of different atomic orbitals to the formation of the valence and conduction bands is approximately identical for pure and alloyed materials. For pure and alloyed materials, the Cu/Ag-d orbital and the S/Se-p orbital are the primary contributors to electronic states near the Fermi energy of the valance band.

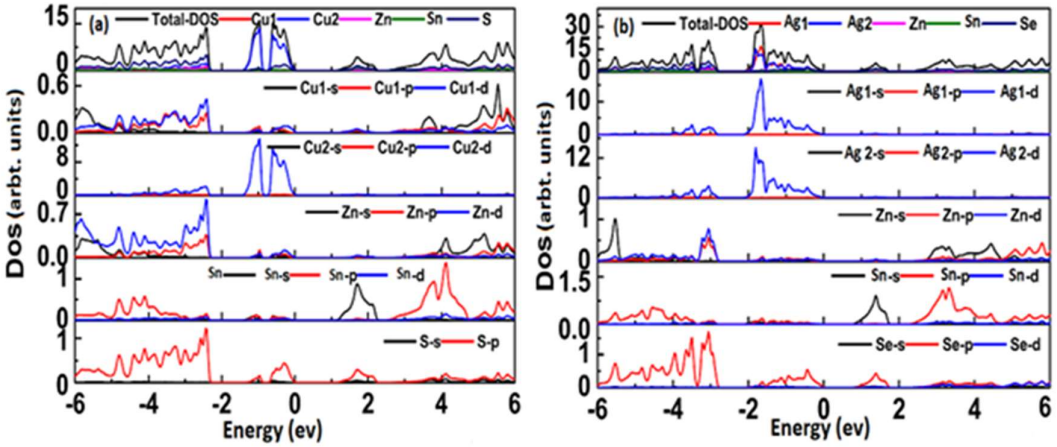

Fig. 2 Total and partial densities of states (DOS) were calculated for (a) pure kesterite Cu_2ZnSnS_4 and (b) alloyed $Ag_2ZnSnSe_4$.

While electronic states in the conduction band at the Fermi energy are dominated by Sn-p and S/Se-p orbitals coupled together, all cations in pure kesterite and alloyed $Ag_2ZnSnSe_4$ have a tetragonal symmetry due to the presence of S/Se atoms. Thus, as long established by their distinct DOS spectra, electronic states are the significance of hybridization of individual cation and anion atomic orbitals [12, 13].

IV. Conclusion

Using the first-principles methods, an alloyed compound of CZTS has been successfully modeled. The compounds were found to show an indirect bandgap characteristic with conduction band minima (CBM) and valence band maxima (VBM) located between the N and gamma points of the Brillouin zone for pure kesterite Cu_2ZnSnS_4 and between the N and A points for alloyed $Ag_2ZnSnSe_4$ respectively. The estimated band gap value for the alloyed was found to be smaller than the bandgap values empirically observed for certain similar alloyed kesterites. This is observed to be consistent with previously published band gap estimates derived from density functional theory.

References

[1] O. António José do Nascimento de, "Nanoparticles in Cu (In, Ga) Se_2 thin film solar cells for light trapping". Ph.D. dissertation, Dept. of Phy. Eng., Fac. of Sci. & Tech., New Univ. of Lis., Lisbon, Portugal, 2019.

[2] Y. Chang *et al.*, "Cu_2ZnSnS_4 solar cells with over 10% power conversion efficiency enabled by heterojunction heat treatment". *Nat. E., vol.* 3, no. 9, pp.764-772, 2018.

[3] European Commission. (2017). Communication from the commission to the European parliament, the council, the European economic and social committee, and the committee of the regions on the 2017 list of Critical Raw Materials for the EU. [Online]. Available: https://eur-lex.europa.eu/legal-content/EN/ALL/?uri=COM:2017:0490:FIN Accessed on: August 14, 2021.

[4] L. Simon *et al.*, "The importance of back contact modification in $Cu_2ZnSnSe_4$ solar cells: the role of a thin MoO2 layer". *Nano E., vol.* 26, pp. 708-721, 2016.

[5] L. Xiaolei, Y. Feng, H. Cui, F. Liu, X. Hao, G. Conibeer, D. B. Mitzi and M. Green, "The current status and future prospects of kesterite solar cells: a brief review". *Prog. in Photovoltaics: Res. & App., vol.* 24, no. 6, pp. 879-898, 2016.

[6] S. Chen, X. Gong, A. Walsh, and S.Wei, "Crystal and electronic band structure of Cu_2ZnSnX_4 (X=S and Se) photovoltaic absorbers: First-principles insights". *App. Phy. Lett., vol.* 94, no. 4, pp. 041903, 2009.

[7] T. Gershon, Y. S. Lee, P. Antunez, R. Mankad, S. Singh, D. Bishop, O. Gunawan, M. Hopstaken and R. Haight, "Photovoltaic materials and devices based on the alloyed kesterite absorber $(AgxCu1–x)_2ZnSnSe_4$." *Adv. E. Mat., vol.* 6, no. 10, pp. 1502468, 2016.

[8] P. P. John, K. Burke and M. Ernzerhof, "Generalized gradient approximation made simple". *Phys. Rev. Lett., vol.* 77, no. 18, pp. 3865, 1996.

[9] M. J. Hendrik and J. D. Pack, "Special points for Brillouin-zone integrations." *Phys. Rev. B, vol.* 13, no. 12, pp. 5188, 1976.

[10] Z. Wei. "A broyden–fletcher–goldfarb–shanno algorithm for reliability-based design optimization, " *App. Math. Model., vol.* 92, pp. 447-465, 2021.

[11] H. Heriche, Z. Rouabaha, S. Benabbesa and L. Selmani, "Thickness optimization of various layers of CZTS solar cell". *J. of New Tech. & Mat., vol.* 277, no. 1747, pp. 1-4, 2014.

[12] G. Galina, J. A. Márquez, A. Franz, C. J. Hages, S. Levcenko, T. Unold and Susan Schorr, "Effect of Ag incorporation on structure and optoelectronic properties of $(Ag_{1–x}Cu_x)_2$ $ZnSnSe_4$ solid solutions". *Phys. Rev. Mat., vol.* 4, no. 5, pp. 054602, 2020.

[13] F. Daniel and S. Schorr, "Climbing Jacob's ladder: A density functional theory case study for $Ag_2ZnSnSe_4$ and $Cu_2ZnSnSe_4$". *J. of Phy. E.,* vol. 3, no. 1, pp. 015002, 2020.